PHYSICAL REVIEW C **69**, 022801(R) (2004)

# New direct study of the $^{19}$Ne$(p,\gamma)^{20}$Na reaction cross section

M. Couder, C. Angulo, E. Casarejos, P. Demaret, P. Leleux, and F. Vanderbist

*Institut de Physique Nucléaire et Centre de Recherches du Cyclotron, Université catholique de Louvain, Louvain-la-Neuve, Belgium*

(Received 19 November 2003; published 23 February 2004)

The $^{19}$Ne$(p,\gamma)^{20}$Na reaction is part of the chain of reactions linking the hot-CNO cycles and the rp-process in hydrodynamic hydrogen and helium burning. The resonance strength of the 448 keV level has been measured in the recoil separator ARES. An upper limit of 15 meV (90% C.L.) has been obtained. This result slightly restricts a prior determination using different methods.

DOI: 10.1103/PhysRevC.69.022801 PACS number(s): 25.40.Lw, 25.60.−t, 27.30.+t

In hydrodynamic H- or He-burning occurring in novae and X-ray bursts, hot-CNO cycles can be escaped to the rp-process through several chains of reactions starting from $^{18}$F:$^{18}$F$(p,\alpha)^{15}$O$(\alpha,\gamma)^{19}$Ne$(p,\gamma)^{20}$Na or $^{18}$F$(p,\gamma)^{19}$Ne$(p,\gamma)^{20}$Na, or $^{18}$F$(\beta^+)^{18}$Ne$(\alpha,p)^{21}$Na [1,2]. Being present in two of them, the $^{19}$Ne$(p,\gamma)^{20}$Na reaction is of great interest. In the temperature domain of relevance in the above environments, the reaction rate is dominated by a resonant level at 448 keV above threshold, at an excitation energy of 2.643 MeV in $^{20}$Na.

This level was produced previously in nuclear reactions induced by stable beams, like $^{20}$Ne$(^3$He$,t)^{20}$Na [3–6] or $^{20}$Ne$(p,n)^{20}$Na [7]. Angular distributions of the tritons suggested a $J^\pi=1^+$ assignment, while the $(p,n)$ reaction data was consistent with a $3^+$ assignment. This level was not observed in the $^{20}$Mg delayed $\beta$-decay [8–10]; as Gamow-Teller $\beta$-decay from a $0^+$ state strongly favors $1^+$ final states, a $1^+$ assignment would require the 2.643 MeV level to be an intruder state. Resonance strengths of 6 meV [4] and 7 meV [5] were calculated. In a microscopic three-cluster model calculation [11], a $J^\pi=1^-$ was attributed to this level, and a resonance strength of 33 meV was calculated. Finally, Brown *et al.* [12] suggested the 2.643 MeV level to be the analog of the 2.966 MeV $3^+$ state in $^{20}$F; from the shell-model-calculated lifetime $(\tau)$ of 3.5 fs for the mirror level, they obtained a resonance strength of 80 meV for the 2.643 MeV state. Adopting the most recent experimental result, i.e., $\tau \leqslant 12$ fs [13], a lower limit of 16 meV was deduced for the resonance strength [14].

Several investigations of the $^{19}$Ne$(p,\gamma)^{20}$Na reaction were performed in Louvain-la-Neuve in the last decade. An upper limit of 21 meV (90% C.L.) was set on the resonance strength of the 2.643 MeV level, when combining the data of two experiments detecting $\alpha$ decays, following $\beta^+$ feeding of high levels in $^{20}$Ne [15]: the detectors used were double-sided silicon strip detectors, and solid-state nuclear track detectors, respectively. Later on, $^{19}$Ne beams of higher energies induced the $(p,\gamma)$ reaction to higher levels above threshold; positrons were detected in a stack of scintillators at the end of a magnetic spectrometer, and resonance strengths were also deduced [16]. All results were summarized and correctly renormalized, and astrophysical consequences were drawn, in a subsequent publication [17].

The above measurements had two drawbacks, i.e., a low detection efficiency, of the order of 1.5%, and the presence of a background from the $^{19}$Ne$(d,n)^{20}$Na competing reaction, induced by the beams on the deuterium present in the $CH_2$ target. The latter imposed an additional measurement on a $CD_2$ target to be made after each $(p,\gamma)$ measurement.

ARES, the Astrophysics REcoil Separator, was built to measure radiative capture reactions of astrophysical interest, in inverse kinematics. ARES is coupled to CYCLONE44 [18], a cyclotron which is used as a postaccelerator to bring radioactive ions to the required energy. The aim in ARES is to separate product ions from beam ions and to detect the former. This separation proceeds in three steps (Fig. 1): (i) the most abundant charge state of the product ions (and of the beam ions at the same time) is selected in a dipole magnet; (ii) a Wien filter or velocity filter transmits the product ions and deflects the beam ions; (iii) a $\Delta E-E$ identification is performed in a $\Delta E$ gas ionization chamber and a $E$ silicon detector of the PIPS type. Extensive tests had been realized for the $^{19}$F$(p,\gamma)^{20}$Ne "mirror" reaction [19]: a resonant state at 635 keV center of mass (c.m.) energy, of 6.2 keV total width and of 1.6 eV resonance strength, had been selected. The main results of these tests are the following: a transmission of 11.5% was measured for the $^{20}$Ne$^{7+}$ product ions (the most abundant charge state); the charge distribution of $^{19}$F and of $^{20}$Ne ions behind the $CH_2$ target was measured and was found in good agreement with the Shima *et al.* [20] calculation; the measured energy distribution of the product ions was fairly well reproduced by a GEANT simulation containing specific energy losses of $^{19}$F and $^{20}$Ne ions in $CH_2$ (the target material) and Isobutane (the gas of the $\Delta E$ counter), which had been previously measured.

In summary a measurement of the $^{19}$Ne$(p,\gamma)^{20}$Na reaction in ARES should benefit from two improvements as compared with previous methods: a slightly larger transmission efficiency ($\sim$4%, from the product of the percentage of the $^{20}$Na$^{7+}$ beyond the target and the transmission of $^{20}$Na$^{7+}$ in ARES) and a suppression of the background from the $(d,n)$ reaction. Simulations of the $^{19}$Ne$(d,n)$ reaction in ARES showed indeed a null transmission of $^{20}$Na$^{7+}$ ions from this reaction.

In the $^{19}$Ne$(p,\gamma)^{20}$Na reaction measurement, a 9.8 MeV $^{19}$Ne$^{3+}$ radioactive beam accelerated by CYCLONE44, was focused on a 80 $\mu$g/cm$^2$ $CH_2$ target. Two PIPS monitors located at forward angle ($\pm 15°$) recorded charged particles scattered by or recoiling from the target. Their time-of-flight with respect to the cyclotron RF and their energy were dis-

 

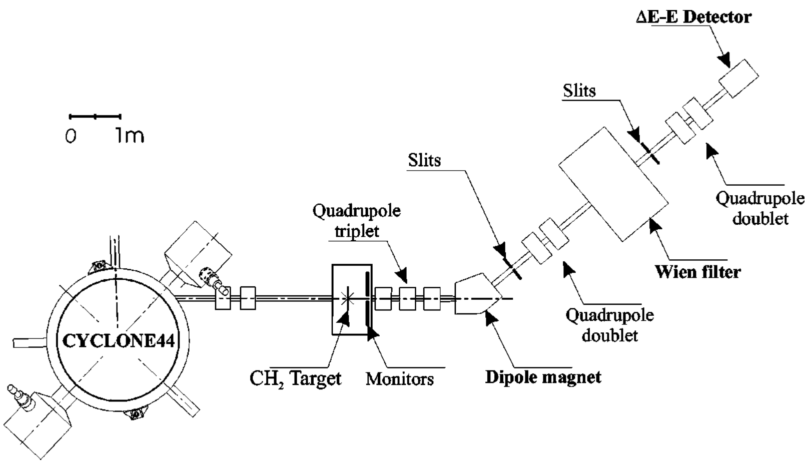


FIG. 1. Layout view of ARES coupled to CYCLONE44.

played in a two-dimensional spectrum permitting particle identification [Fig. 2(a)]. The recoil proton spectra are of particular interest [Fig. 2(b)]. As the resonance width is smaller than the lower limit ($\sim$0.5 keV, see Ref. [21]) able to distort in a significant way the classical Coulomb pattern, proton spectra were fitted with a Rutherford cross section. The fit provided with the product of the Hydrogen content in the target and the integrated beam intensity. Working with a low intensity radioactive beam, no hydrogen loss is expected and a 2-to-1 stoecheometry was assumed throughout the experiment (different targets were used), leading to an average $^{19}$Ne$^{3+}$ beam on target equal to $(1.08\pm 0.11)10^{8}$ pps. Another specific part of the proton spectra, i.e., the upper edge, allowed to deduce the incident beam energy on target (let us recall that high-energy protons are produced by the beam in the front face of the target). Regarding the radioactive beam itself, two other characteristics were measured as follows.

(i) *The beam purity*. It is well known that radioactive beams produced by the ISOL-method can be contaminated by a stable isobar. The $^{19}$Ne beam with a reduced intensity was transported through ARES and identified in the $\Delta E$-$E$ telescope. The contamination in $^{19}$F was at most 0.7%.

(ii) *The beam energy distribution on target*. This information is an important input to the simulation code, which will eventually furnish the transmission efficiency of the $^{20}$Na product ions. A full width at half maximum (FWHM) of the $^{19}$Ne beam equal to 260 keV was measured in a PIPS detector at the target place. This number is much larger than the FWHM of a stable $^{19}$F beam at the same energy (170 keV), indicating that the tuning of CYCLONE44 to maximize both the $^{19}$Ne-$^{19}$F separation and the $^{19}$Ne acceleration efficiency leads to a degradation of the beam quality.

The beam energy had been adjusted so that $^{20}$Na ions from the resonant state were produced at about 60 $\mu$g/cm$^2$ from the front face of the target; the thickness that they had to cross before leaving the target was sufficient to reach the equilibrium of the charge states.

In order to transmit properly $^{20}$Na ions through ARES, their energy behind the target has to be known. Discrepancies among stopping power tables lead us to measure the stopping power for $^{20}$Ne and $^{23}$Na in $CH_2$, and also in isobutane, as we did before for $^{19}$F and $^{20}$Ne in the test reaction.

Coming now to the $^{19}$Ne$(p,\gamma)$ measurement, ARES was tuned as follows: the $^{19}$Ne$^{7+}$ beam was transported through ARES, all the elements being optimized successively. Typical transmission of 60% was obtained. Then, knowing the energy of $^{20}$Na ions behind the target, the dipole field and the Wien filter magnetic field were changed accordingly to transport $^{20}$Na ions to the $\Delta E$-$E$ detector. About 500 $^{19}$Ne$^{7+}$ were transmitted per second as well, the rejection factor of the $^{19}$Ne beam being typically equal to $5\times 10^{-6}$. This is roughly a factor of 10 worse than the one obtained in the $^{19}$F$(p,\gamma)^{20}$Ne test reaction. The lower quality of the radioactive beam is probably the reason for that.

The counting rate of the $\Delta E$-$E$ coincidence was limited to a few hundred Hz, in order to limit pile-up of $^{19}$Ne events extending into the region of the $\Delta E$ vs $E+\Delta E$ plane where $^{20}$Na events were expected. The $\Delta E$ gas counter was operated at a pressure of 4 mb isobutane. Figure 3 presents a two-dimensional spectrum of the $\Delta E$ vs $E+\Delta E$ events. The dark area is the region of the $^{19}$Ne ions. A solid line surrounds the region of the $^{20}$Na ions, which was determined from a simulation of $^{20}$Na events tracked through ARES from the target to the $\Delta E$-$E$ detector. The measured stopping power of $^{23}$Na ions in $CH_2$ and in isobutane was part of the simulation. Two regions of equal surface were selected right and left to the region of interest (ROI). Pile-up events, occurring in these regions at a level of $10^{-7}$ of the leaky beam events, were summed and the mean of the counts in both regions was subtracted from the counts in the ROI.

The remaining counts were corrected for the efficiency of the setup, which is the product of two factors, the amount of $^{20}$Na$^{7+}$ ions after the target, and the transmission of $^{20}$Na$^{7+}$ in ARES. The first factor (0.37) was obtained from Shima's tables [20], which had been checked for $^{19}$F and $^{20}$Ne ions, and had been found in agreement with our measurements, at least for the most abundant state, i.e., $7^+$ [19]. The second factor was deduced from a simulation of $^{20}$Na$^{7+}$ ions tracked from the target to the $\Delta E$-$E$ telescope. The global efficiency was 2.7%. It is justified to suppose that the observed yield is from the 2.643 level in view of the very small contribution expected from direct capture [16]. The resonance strength $\omega\gamma$ is then given by

$$\omega\gamma = \frac{Y}{I}\frac{2}{\lambda^2}\epsilon_{lab}\frac{m_t}{m_t+m_p},$$

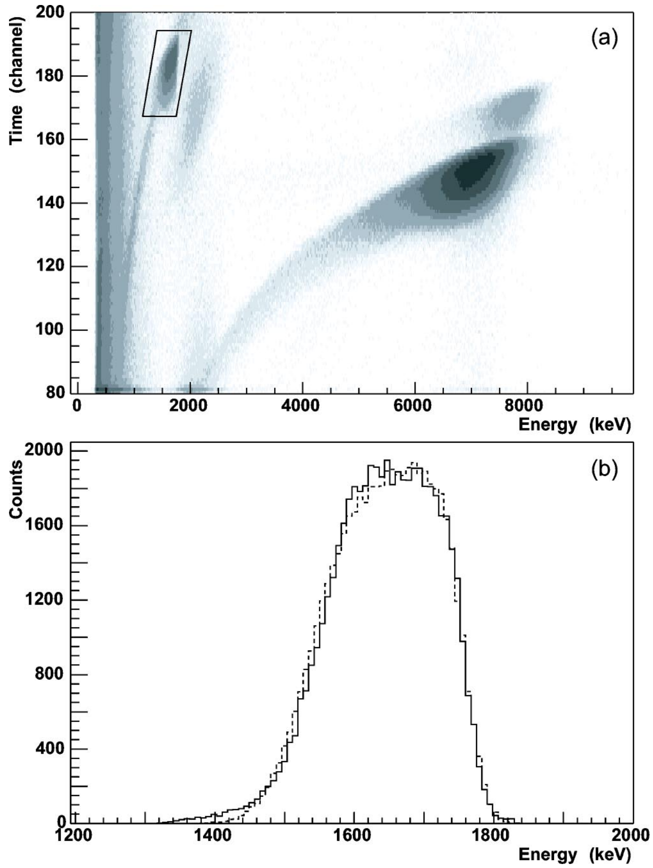


FIG. 2. (a) Two-dimensional spectrum, time-of-flight vs energy, for particles recorded in a silicon detector at +15°, resulting from interactions of $^{19}$Ne beam ions and a $CH_2$ target. Regions corresponding to scattered $^{19}$Ne and recoil $^{12}$C are clearly visible in the high-energy region. The proton region is encircled. A parasitic $^{19}$Ne beam of low energy and low intensity ($\leqslant$1% of the main beam) accelerated by the cyclotron appears to the right of the proton region. The low-energy pulses showing no correlation with the cyclotron RF are positron events. (b) The projection of the proton region to the energy axis (solid histogram) is shown. The dotted histogram is a fit.

where $Y$ is the number of $^{20}$Na events corrected for the efficiency, $I$ is the integrated $^{19}$Ne beam intensity, λ is the c.m. wave length (in cm$^2$), $\epsilon_{lab}$ is the stopping power of $^{19}$Ne ions in $CH_2$ (in $10^{-15}$ eV cm$^2$/at), $m_t(m_p)$ is the mass of the target (of the projectile), in a.m.u.

The final result is $\omega\gamma = -1.0 \pm 9.6$ meV. To the 9.6 meV statistical error a systematic uncertainty should be added. The latter comprises the uncertainty to the integrated beam and to the transmission of ARES: the first one was estimated above, while the second one was obtained by changing in the simulation code the slits positions by 0.5 mm (dipole exit and Wien filter exit) and taking extreme values of the efficiency. A systematic uncertainty of 0.6 meV was deduced.

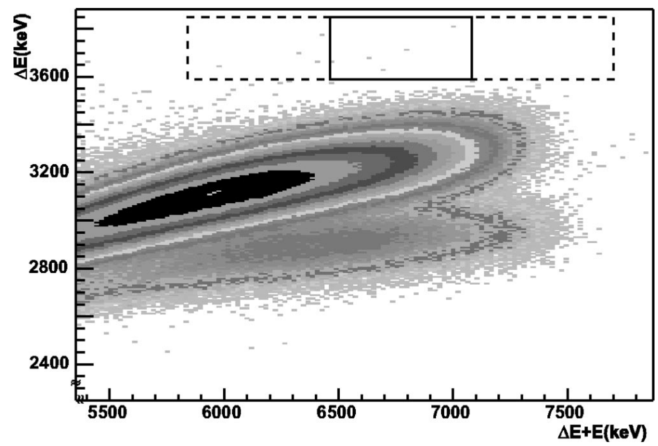


FIG. 3. Two-dimensional spectrum, $\Delta E$ vs $E+\Delta E$, in the end detectors of ARES for the $^{19}Ne(p,\gamma)^{20}Na$ reaction. The count scale is logarithmic in intensity. The dark area consists in $^{19}$Ne leaky beam events. The leaky $^{19}$F contaminant beam events are visible just below the $^{19}$Ne region. The framed area limited by solid lines is the expected location for $^{20}$Na events from the 2.643 MeV level. Adjacent regions limited by dashed lines are used to estimate the background. See text for more details. This figure is a typical run. During the experiment, changes of target, of ARES settings and of $\Delta E$ gas pressure resulted in different locations for $^{20}$Na events.

Both types of uncertainties were combined in quadrature, the positive part of the Gaussian distribution of the result was renormalized to 1, and an upper limit of 15.2 meV (90% C.L.) was obtained. This value reduces slightly the upper limit from our first experiment [17], it is in agreement with the first prediction of 6 meV or 7 meV for a $1^+$ state [4,5], and does not contradict (at a $2\sigma$ level) the most recent calculated lower limit of 16 meV for a $3^+$ state [14].

In summary, a new measurement of the resonance strength of the 2.643 MeV level was performed with a recoil mass separator. This measurement restricts a previous one obtained with quite different methods. Significant improvements of the ARES transmission and efficiency are required to yield more than an upper limit to the 2.643 MeV level. Some of them are presently examined.

We wish to thank M. Jacques for the installation of the remote control of ARES, G. Tabacaru, W. Galster, J.-S. Graulich and S. El Hajjami for preliminary tests of ARES, and Ch. Delaere for help during the experiment. The staff of the Cyclotron Research Center is acknowledged for the very reliable operation of CYCLONE44 in this first experiment with a radioactive beam. One of us (P.L.) is a Research Director of the National Fund for Scientific Research, Brussels. This paper presents results of the Belgian Programme on Interuniversity Attraction Poles initiated by the Federal Policy Office, Brussels. Scientific responsibility is assumed by the authors.

[1] R. K. Wallace and S. E. Woosley, Astrophys. J., Suppl. Ser. **45**, 389 (1981).
[2] M. Wiescher, J. Görres, and H. Schatz, J. Phys. G **25**, R133 (1999).
[3] S. Kubono *et al.*, Z. Phys. A **331**, 359 (1988).
[4] L. O. Lamm *et al.*, Nucl. Phys. **A510**, 503 (1990).
[5] M. S. Smith *et al.*, Nucl. Phys. **A536**, 333 (1992).
[6] J. Görres and M. Wiescher, Phys. Rev. C **52**, 412 (1995).
[7] B. D. Anderson *et al.*, Phys. Rev. C **52**, 2210 (1995).
[8] S. Kubono *et al.*, Phys. Rev. C **46**, 361 (1992).
[9] J. Görres *et al.*, Phys. Rev. C **46**, R833 (1992).
[10] A. Piechaczek *et al.*, Nucl. Phys. **A584**, 509 (1995).
[11] P. Descouvemont and D. Baye, Nucl. Phys. **A517**, 143 (1990).
[12] B. A. Brown *et al.*, Phys. Rev. C **48**, 1456 (1993).
[13] J. Görres *et al.*, Phys. Rev. C **50**, R1270 (1994).
[14] H. T. Fortune *et al.*, Phys. Rev. C **61**, 057303 (2000).
[15] R. D. Page *et al.*, Phys. Rev. Lett. **73**, 3066 (1994).
[16] C. Michotte *et al.*, Phys. Lett. B **381**, 402 (1996).
[17] G. Vancraeynest *et al.*, Phys. Rev. C **57**, 2711 (1998).
[18] G. Ryckewaert *et al.*, Nucl. Phys. **A701**, 323c (2002).
[19] M. Couder *et al.*, Nucl. Instrum. Methods Phys. Res. A **506**, 26 (2003).
[20] K. Shima *et al.*, At. Data Nucl. Data Tables **51**, 173 (1992).
[21] R. Coszach *et al.*, Phys. Rev. C **50**, 1695 (1994).